

UNIVERSITÄT LEIPZIG

Fakultät für Physik und Geowissenschaften  
Institut für Meteorologie  
Arbeitsgruppe Wolken und Globales Klima

## Bachelorarbeit

zum Erwerb des akademischen Grades

## Bachelor of Science

Thema

# Influence of aerosols and greenhouse gases on time of emergence of climate change signal in mean and extreme regional surface temperature

vorgelegt von

Felix Fauer

Gutachten:

Johannes Quaas  
Marc Salzmann

Leipzig, Oktober 2017

## Abstract

This Bachelor thesis is about the influence of aerosols on the time at which surface temperature is outside of natural variability for the first time (Time of Emergence, TOE). The comparison of time series alone does not satisfy a climate change investigation because it does not pay regard to natural variability which can lead to extreme events. That is why the signal of climate change is analyzed depending on its relation to model control runs where all anthropogenic emissions are constant at the state of 1850. The variability range of control runs is used as confidence interval for natural variability. When a signal leaves the confidence interval for at least 4 consecutive years, this is defined as TOE.

Those TOE are calculated from results of several Coupled Model Intercomparison Project - Phase 5 (CMIP-5) models for the years from 1850 to the end of 2005. Each model is run for two different scenarios where only greenhouse gases (GHG) or both greenhouse gases and aerosols (HISTorical) are taken into account. The majority of those models comprise several realizations. TOE from these realizations are averaged and presented as one model TOE for each model.

Aerosols are assumed to have a cooling influence on global climate. That is why TOE is expected to arise earlier in a hypothetical case where there are no anthropogenic aerosol emissions. A focus of this thesis is on the increased European aerosol emission in the 1950s and whether they caused a delay in the occurrence of TOE. Based on statistical analysis in Europe the model-averaged TOE for mean temperature is shifted by about  $29.5 \pm 41.8$  years towards the past when aerosol emissions are disabled. The difference between HIST and GHG in years will be used as a measure of aerosol influence in different models and for different continents, outside of Europe as well. In every region, the mean temperature TOE for experiments including only greenhouse gases (GHG) happens earlier than in the historical (HIST) experiment. The same applies to maximum temperature in most but not all regions. It is important to notice, that TOE could be sensitive to details of their definition. Those details were set in a mix of parameter adjustments and reasonable choices based on comparison to literature.

# Contents

<b>1</b>	<b>Introduction</b>	<b>4</b>
<b>2</b>	<b>Methods</b>	<b>5</b>
2.1	CMIP-5 Project . . . . .	5
2.2	Calculations . . . . .	5
2.3	Confidence Interval . . . . .	6
2.4	Time of Emergence . . . . .	7
2.5	Observations . . . . .	9
<b>3</b>	<b>Results</b>	<b>10</b>
3.1	Parameter adjustment for TOE . . . . .	10
3.2	Influence of aerosols . . . . .	11
3.3	Regional variability . . . . .	14
3.4	Differences in models . . . . .	16
3.5	Reliability of CMIP5 models . . . . .	20
<b>4</b>	<b>Discussion</b>	<b>22</b>
4.1	Possible causes of disagreement . . . . .	22
4.2	Conclusion . . . . .	22
<b>5</b>	<b>Outlook</b>	<b>23</b>

# 1 Introduction

The influence of aerosols still has a high uncertainty in global climate models (GCM), but most studies agree that there is a negative total aerosol forcing. Especially in the years 1950-1980 the Earth's surface received a decreasing amount of radiation, which is called "dimming" phase (Allen et al., 2013). The most probable reason are indirect aerosol effects (Stanhill and Cohen, 2001), which also caused a decrease in global mean temperature in this time. Mitchell et al. (1995) investigated aerosol influence by comparing different GCM experiments where aerosols can be switched on and off. Their findings suggest an increase in global warming, when positive greenhouse gas forcing further dominates negative Aerosol forcing. They also reconstructed the European 1960 temperature drop due to increased aerosol emissions. Boer et al. (2000) extended the simulation range to the year 2100 and expect a global mean temperature difference of 1.2°C between aerosol-forced and GHG-only model experiments for the year 2100.

The analysis of signals leaving the background noise range is an important approach in climate modelling, because it takes the natural variability into account, which is also able to cause extreme phenomenons. Many socioeconomic problems do not arise from parameter changes itself but from changes that leave range of natural variability (Lobell and Burke, 2008). This is because adaptation of human and natural systems is related to variability ranges more than to absolute optimum values.

Warming is expected to occur in high latitudes to a higher extent but also with larger variability and at later time points than in low latitudes (Mahlstein et al., 2011). In this thesis, it will be analyzed whether TOE signals support this theory and are delayed accordingly in high latitudes although the defined regions may not be adequate for this kind of investigation (see Chapter 3.3).

Hawkins and Sutton (2012) studied TOE in different GCMs and created global maps with regional analyzes. They found TOE delays of several decades between different regions, especially for mid latitudes. Their focus is on the high uncertainty of this kind of investigation which can be up to 60 years.

While this study concentrates on the past, there are also simulations that make assumptions about the aerosol impact on extreme weather events under different future scenarios. Future extreme events like tropical nights, temperature records and precipitation amounts which can be combined under the term 'heat waves' are more likely to occur in a climate with a maximum decrease of aerosols (Sillmann et al., 2013).

A new aspect of the present study is the investigation of modelled TOE differences between historical (Aerosol+GHG) and GHG-only experiments for a time range in the past. Especially the 1950 aerosol emission increase in Europe may have forced a delay in climate change signals. Also the mean temperature development is compared with maximum temperature development, in order to include extreme events as an indicator of global warming. It will be analyzed, at which time point the signal leaves the background noise for at least 4 consecutive years which represents the TOE. Background noise is generated by control runs with fixed aerosol and greenhouse gas emissions of 1850. The 5<sup>th</sup> and 95<sup>th</sup> percentile of those control runs mark the borders of background noise. More detail about the underlying calculations are given in Chapters 2.3 and 2.4.

Table 1: List of CMIP5 models included in TOE analysis

Center	Model	Realizations (Hist/GHG)	grid size	Reference
CCCma	CanESM2	5 / 5	64 × 128	Arora et al. (2011)
CNRM- CERFACS	CNRM-CM5	10 / 6	128 × 256	Voltaire et al. (2013)
CSIRO-QCCCE	CSIRO-Mk.3-6-0	10 / 10	96 × 192	Collier et al. (2011)
IPSL	IPSL-CM5A-LR	6 / 6	96 × 96	Dufresne et al. (2013)
MIROC	MIROC-ESM- CHEM	1 / 1	64 × 128	Watanabe et al. (2011)
MIROC	MIROC-ESM	3 / 3	64 × 128	Watanabe et al. (2011)
MOHC	HadGEM2-ES	4 / 4	145 × 192	Bellouin et al. (2011)
MRI	MRI-CGCM3	5 / 1	160 × 320	Yukimoto et al. (2012)
NCC	NorESM1-M	3 / 1	96 × 144	Bentsen et al. (2012)
NOAA-GFDL	GFDL-CM3	5 / 3	90 × 144	Donner et al. (2011)

## 2 Methods

### 2.1 CMIP-5 Project

The Coupled Model Intercomparison Project Phase 5 (CMIP5) is an attempt to compare climate models under similar boundary conditions. Since every model contains slightly different parametrizations, the diverging outputs give hints about the impact of mechanisms on future and past climate changes. In Table 1 all analyzed models are listed together with their number of different realizations, grid size and their authors. Only those CMIP5 models with control runs longer than 256 years are included, because the calculation of the variability range according to Chapter 2.3 does not work with shorter control runs.

### 2.2 Calculations

Two different parameters are defined: yearly mean temperature (MEAN) and yearly maximum temperature (MAX). All model analysis is based on daily mean surface temperatures. MEAN is defined as the average of daily mean temperature over all grid points inside the respective region and over all days of one year. MAX is defined as the highest daily mean temperature of one year inside the respective region. Note that MAX does not contain daily maximum temperatures and that MAX values of all grid points inside a region may tend to occur within a small subregion of the defined regions. MAX temperature is also a measure of extreme events, pointing out heat.

All models in the ensemble work on a regular grid. So the cell area is not constant on different latitudes. MEAN calculations are weighted with the area of one cell whereas Maximum values are not depending on grid size and therefore are not weighted.

Nine regions for which the TOE is calculated are defined in order to distinguish regional differences. They are listed in Table 2. Those regions are mainly based on continental land borders but have a rectangular shape. Grid points with an assigned land fraction of less than 50% are excluded from the analysis. However, there is one exception for the Arctic region where all grid points with a latitude higher than  $66.6^\circ$  are included, since there is no land mass around the Earth’s North Pole. Please note that some continents like Europe or the Middle East have a

Table 2: **List of regions, their extent and boundaries.** Because of the different grid sizes in models, the number of grid points is listed with a minimum value of the model with the highest grid size and mean and maximum value respectively.

Region	number of grid points (Min/Mean/Max)	Boundary Coordinates (Lat/Lon) in degree
Africa	356 / 843 / 2274	-168 ... -17 / 17 ... 90
Antarctic	767 / 1907 / 5047	-17 ... 53 / -50 ... 36
Arctic	1024 / 2490 / 6720	0 ... 0 / 66 ... 90
Asia	734 / 1721 / 4707	29 ... 73 / 8 ... 38
Australia	92 / 212 / 567	80 ... -130 / -60 ... -11
Europe	127 / 304 / 806	-14 ... 40 / 36 ... 70
Middle East	114 / 266 / 720	-100 ... -25 / -60 ... 17
North America	473 / 1112 / 3066	40 ... -168 / -11 ... 90
South America	207 / 475 / 1255	0 ... 0 / -90 ... -60

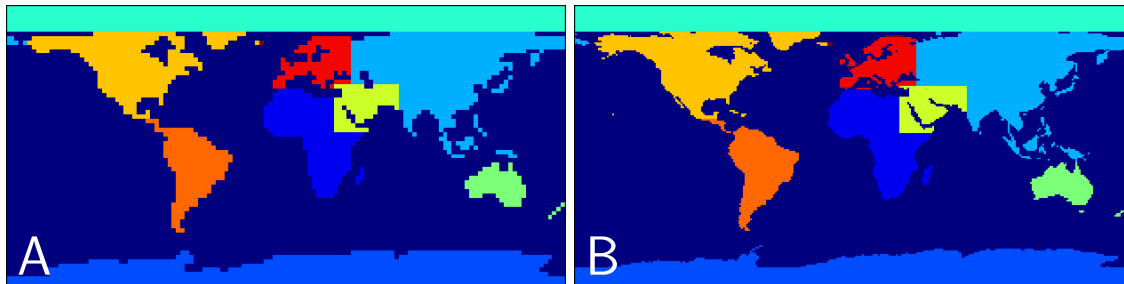


Figure 1: **Region boundaries.** Each of the CMIP5 models has a different grid size. The model with the largest grid size is MIROC-ESM (A) and the smallest is MRI-CGCM3 (B).

smaller area than others which leads to differences in the statistical relevance of mean values. All models have varying grid sizes, so the borders between regions may differ a little. Also, Hourdin et al. (2013) found that a change of grid size (in case of IPSL-CM5A) has potential to change model results when it comes to the future development of temperature. As a representative, the resulting maps of models with the smallest (MIROC-ESM) and the highest (MRI-CGCM3) resolution are displayed in Figure 1.

### 2.3 Confidence Interval

Here, a 90% confidence interval defines the boundaries for natural variability. These boundaries are based on control simulation runs with a fixed aerosol and greenhouse gas emission from 1850. The construction of a variability range which will be explained in the following passage, is also visualized in Figure 2.

Control runs have an extent of several hundred years mostly. Most of the actual model (not control) runs comprise exactly 156 years (1850-2005). That is why as much as possible slices with a length of 156 years are extracted from the control runs, each shifted by 5 years. Then, those slices have been aligned to always match the first year of each slice. For each year the 5<sup>th</sup> percentile of all aligned slices defines the lower and the 95<sup>th</sup> percentile defines the upper limit for natural variability. The probability of exceeding the upper bound of the 90%-confidence interval

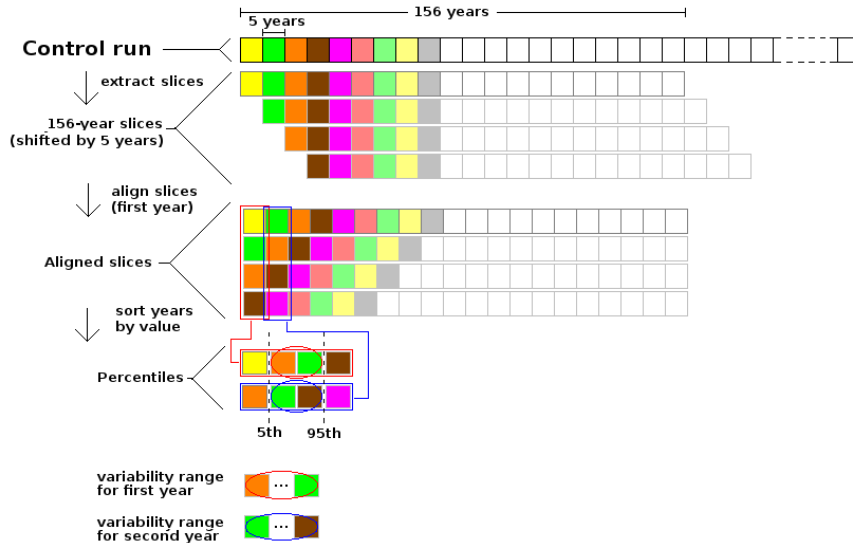


Figure 2: **Variability range.** Natural variability range is deduced from noise in control runs. Each color represents a temperature value. In this Figure, five years are condensed to one color, only for clarity. All aligned values between the 5<sup>th</sup> and 95<sup>th</sup> percentile are defined as variability range of one year. All included models contain a sufficient amount of years to enable at least 20 slices which are necessary to calculate both percentiles.

(95<sup>th</sup> percentile) by coincidence for each year will be

$$p_1 = \frac{1}{20}. \quad (1)$$

This approach can be used, because all models contain enough years to make at least 20 slices possible. The minimum length of a control run is 256 years. This length results from the basic length of each experiment (156 years) added to the number of slices (at least 20) times the shift for each slice (5 years), shown in Equation 2.

$$156 + 20 \cdot 5 = 256 \quad (2)$$

All models from the CMIP5-project that provide an insufficient number of years (<256) in the control run, are excluded from the analysis and are not listed in Table 1.

## 2.4 Time of Emergence

Many different definitions exist for the term "time of emergence" (TOE). For Giorgi and Bi (2009) a TOE arises when the signal exceeds the background noise limits. Hawkins and Sutton (2012) used TOE as the time when the signal-to-noise ratio becomes higher than a certain threshold which can be 1.0 or higher. A threshold of 1.0 would be equal to Giorgi's definition of TOE. Another definition is stated by Bador et al. (2016) who look for signals that leave natural variability for several ( $m$ ) consecutive years.

At first an approach where  $m$  out of 10 years need to be outside the confidence interval to satisfy a TOE is investigated within this thesis's work. The encounter of TOE become very coincidental

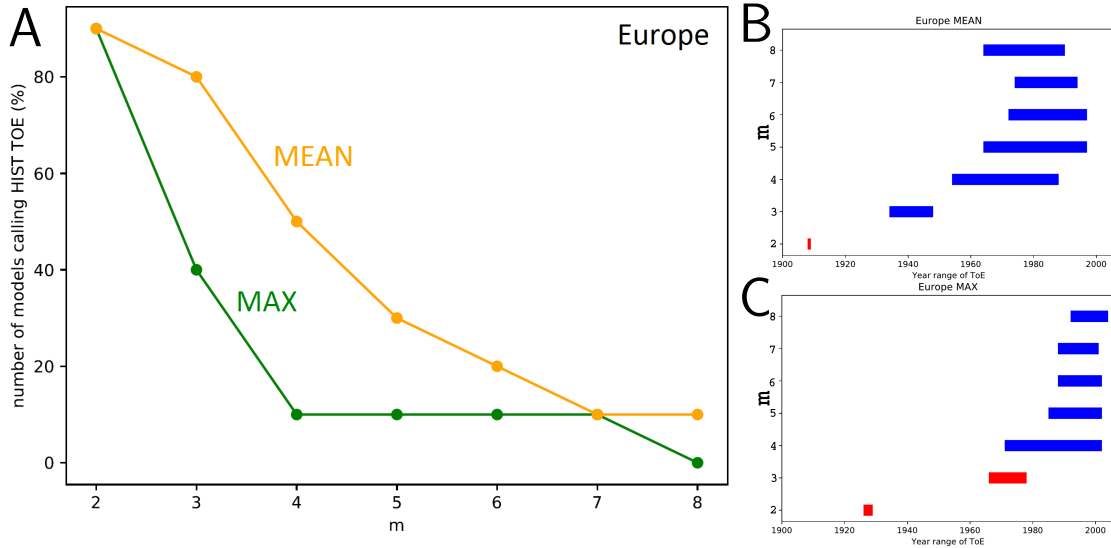


Figure 3: **Parameter adjustment for  $m$  in Europe.** The parameter  $m$  determines for how many consecutive years a signal needs to be outside of the confidence interval in order to call a TOE. For both Figures, results from 10 models and all of their realizations are included. The TOE results of all realizations are averaged. **A:** number of MAX and MEAN TOE for each parameter  $m$  normalized to the maximum possible number of HIST TOE, which is 10 (equal to the number of models). **B:** MEAN TOE range for Europe. Blue bars indicate the average TOE (of all models and realizations which call a TOE) with their GHG year on the left and HIST year on the right end of the bar. Red bars indicate GHG years on the right and HIST years on the left end. **C:** MAX TOE range for Europe.

and TOEs are called, when no significant warming is visible. That is why this approach will be rejected and the TOE definition with  $m$  consecutive years (Bador et al., 2016) will be used instead.

Some TOE might occur coincidentally without necessarily indicating a significant climate warming. It does not make sense to calculate the mean temperature time series of all realizations in one model, because the number of realizations is different for each model (see Table 1) and different model's results would lose their comparability to each other. Moreover, TOE-influencing events that last for several years in one realization may be shifted by a few years in another realization. In such a case, those event could disappear in the averaging process. For this reason, not time series but TOE years will be averaged over different realizations. Furthermore, a valid TOE for this model will be called only, when at least half of its realizations call a TOE. If there are too few TOE for a specific  $m$ , the value of  $m$  will be increased gradually until at least half of the model's realizations find one TOE for  $n \geq m$ . Then, all found TOE will be averaged. That way, in the average TOE year for  $m$  there may be some TOE years included, that were called after  $n > m$  years, in order to reach the minimum number of realizations. However, this procedure is only applied to the actual TOE analysis. During the parameter adjustment  $m$  is fixed to the given value and is not increased gradually.

The value for  $m$  was determined in a parameter adjustment. Detailed results of this adjustment are explained in Chapter 3.1. Since this thesis focuses on European TOE, here in the methods section only European MAX and MEAN values are shown (see Figure 3).

It is important to find a value for the parameter  $m$  which satisfies certain conditions. On the



one hand it should not be too high because then very few TOE will arise and an analysis is not meaningful. The number of models that call a HIST TOE within modeling time span decrease with higher  $m$ -values (see Figure 3A). The harder the TOE condition becomes, the less TOE occur. If  $m$  is too small, many TOE will arise very early, often before the year 1900. Those early TOE do not comply with this thesis’s intention to investigate the aerosol delay effect in the 1950s. Harder TOE conditions cause a shift of all TOE (both HIST and GHG) towards later time points, as can be seen in Figure 3B.

It seems reasonable to agree on a value  $m = 4$  consecutive years. Smaller values cause TOE before the year 1950 (see Figure 3B), which are not wanted, because we focus on events after 1950. Those TOE may have high coincidental influence. Higher values of  $m$  inhibit the encounter of TOE to much (see Figure 3A).

The chance  $p$  of one year being warmer than the 95<sup>th</sup> percentile is  $p_1 = 1/20$ . The probability  $p_4$  of exceeding the upper bound of the 90 %-confidence interval (5<sup>th</sup> to 95<sup>th</sup> percentile) by coincidence (in a non-changing climate) for  $m = 4$  consecutive years is

$$p_4 = \left(\frac{1}{20}\right)^4 = \frac{1}{160000} = 6,25 \cdot 10^{-6}. \quad (3)$$

However, this calculation has to be treated with caution, because one year’s MEAN or MAX temperature is depending on the previous year’s temperature. So, the probability  $p_4$  may be higher, than stated in Equation 3.

## 2.5 Observations

Measurement data has been obtained from the HadEX2 Dataset project. They collected data from about 7000 temperature and 11,000 precipitation stations all over the globe and collocated them onto a  $3.75^\circ \times 2.5^\circ$  grid in order to make it comparable to the results of climate modelling. Data has been obtained for the years 1901 to 2010 (Donat et al., 2013). Unfortunately, there are huge differences in availability of data because of orographic or political barriers. That is why some areas have to be interpolated to a great extent. Because many data stations were added during the measurement time since its start in 1901, the number of available data points is continuously growing, even within defined partial regions. That leads to uncertainties especially in the first recorded years, when the amount of data points is comparatively small and may refer to more biased parts of the corresponding region. The used measurement data contain only values for the hottest day in a year (TXx, yearly maximum value of daily maximum temperature) (Donat et al., 2013) in contrast to the model data, that is used in this thesis.

Table 3: **Number of encountered TOE depending on adjustment parameter  $m$  (in %)**. Ratio of encountered TOE compared to the maximum possible number of TOE that can be found. Since there are 10 different models and 2 experiments (HIST and GHG) for each model, the maximum possible number for both is 20 (100%). The maximum possible number for only HIST is 10 (100%). The TOE of all realizations are averaged according to Chapter 2.4.

$m$	MAX				MEAN			
	world		Europe		world		Europe	
	both (HIST and GHG)	HIST	both	HIST	both	HIST	both	HIST
2	90	90	95	90	90	90	95	90
3	60	50	60	40	90	90	80	80
4	40	20	35	10	85	90	70	50
5	35	10	35	10	80	80	55	30
6	35	10	25	10	75	80	50	20
7	30	10	20	10	70	80	30	10
8	15	10	15	0	60	70	15	10

### 3 Results

#### 3.1 Parameter adjustment for TOE

A major problem is to find a value for  $m$  that gives models the chance to encounter a TOE within modelled time span until end of 2005. With increasing  $m$  the number of models gaining a TOE decreases (see Figure 3). When more consecutive years outside the confidence interval are required to call a TOE, the TOE condition becomes stronger. That reduces the chance to achieve a TOE.

Due to the cooling effect of aerosols, in most models GHG TOE occur more often before the year 2005 than HIST TOE. For this reason in Table 3 the ratio of encountered HIST TOE is listed separately next to the ratio of encountered TOE in total (both HIST and GHG). For MEAN TOE, there is even up to  $m = 6$  a possibility to encounter a HIST TOE in 20% of all models in Europe and 80% in the whole world. In MAX TOE analysis it is harder to find a TOE. Even for a comparatively small value of  $m = 4$  only 10% of all models (which is exactly one model) find a HIST TOE in Europe and 20% in the whole world.

The strength of a TOE condition regarding the  $m$ -value can also be seen in the average TOE in Table 4. TOE are shifted to later time points with increasing  $m$ . For small  $m \leq 2$  especially in Europe TOE are called early. Those TOE are not suitable to investigate the 1950 aerosol effect.

However, with higher  $m$  the increase in TOE year becomes smaller. When changing from  $m = 7$  to  $m = 8$  the TOE is shifted only by a few years in most cases. In some cases it even is shifted towards the past. This can be a first proof for modelled climate events occurring outside of natural variability, because the indicator (TOE) becomes more independent of the parameter  $m$  from a certain strength level on.

In very few cases an increase of  $m$  leads to earlier TOE. This can happen, when one or more models with a late TOE are excluded from the average TOE because the TOE condition becomes too strong to allow those late TOE. Those models were included in the weaker TOE condition and enlarged the average TOE.

For all further analysis, a value of  $m = 4$  will be used, as explained in Chapter 2.4.

Table 4: **Average TOE depending on  $m$ .** Each TOE is an average of all found TOE in all 10 models. The TOE of all realizations are averaged according to Chapter 2.4.

$m$	MAX				MEAN			
	world		Europe		world		Europe	
	GHG	HIST	GHG	HIST	GHG	HIST	GHG	HIST
2	1935	1920	1929	1926	1887	1873	1909	1908
3	1959	1962	1978	1966	1899	1909	1934	1948
4	1965	1964	1971	2002	1897	1930	1954	1988
5	1979	1971	1985	2002	1905	1930	1964	1997
6	1979	1971	1988	2002	1915	1933	1972	1997
7	1979	1997	1988	2001	1922	1932	1974	1994
8	1980	1997	1992	2004	1927	1937	1964	1990

### 3.2 Influence of aerosols

In direct comparison of those model experiments containing aerosols and greenhouse gases (henceforth HIST) and those containing only greenhouse gases (GHG) differences can be seen. In Figure 4 all four time series of the MEAN and MAX temperature anomaly relative to the mean of 1860-1890 are shown. The GHG curve shows a steadily rising MEAN temperature whereas in HIST MEAN (see Figure 4A) there are interruptions with cold phases at several points in time. Some of those interruptions can be explained by volcano eruptions, namely Santa Maria (1902), Novarupta (1912), El Chichon (1982) and Pinatubo (1991). A long lasting local HIST temperature minimum appears in the years 1965 until 1975, both in Figures 4B and D. The reason for this can be found in the massively increased aerosol emission in the 1950s, especially in Europe but also North America and parts of Asia (Smith et al., 2011). In the GHG experiment all models end with a higher temperature anomaly in 1995-2005 than in the corresponding HIST experiment. This is because of the aerosol’s cooling influence which is included in the models. The lowest temperature increase in the MEAN (see Figure 4A) and MAX GHG (4B) experiment was modelled by NorESM1-M, the highest increase by GFDL-CM3. Notably, the GFDL-CM3 model also ends with the lowest MEAN HIST temperature anomaly (4D) in the MEAN experiment. This corresponds to the large dimming effect in this model, found by Allen et al. (2013). The highest increase in both HIST experiments (4C and 4D) is shown by IPSL-CM5A-LR. All models (GHG and HIST) show a distinct positive temperature anomaly relative to 1860-1890.

One of the main goals is to investigate whether rise of temperature (MEAN and MAX) with or without aerosols occurs within natural variability or not. Therefore TOE are compared, which indicate the year, when a signal first leaves the 90% confidence interval for at least 4 consecutive years in at least half of all available realizations. The choice of 4 years is discussed in the Chapters 2.4 and 3.1.

The results of MEAN TOE comparison are shown in Figure 5A. In most of the models the MEAN GHG TOE (if any) occur previous to MEAN HIST TOE (blue bar). That result of the majority of models is caused by the cooling aerosol effect. The differences for HIST and GHG TOE range from -25 years (CNRM-CM5) to 62 years (HadGEM2-ES).

Only in two models (NorESM1-M and CNRM-CM5) MEAN HIST TOE is reached past MEAN GHG TOE, indicated by a red bar, which means that aerosols force MEAN temperature to exceed

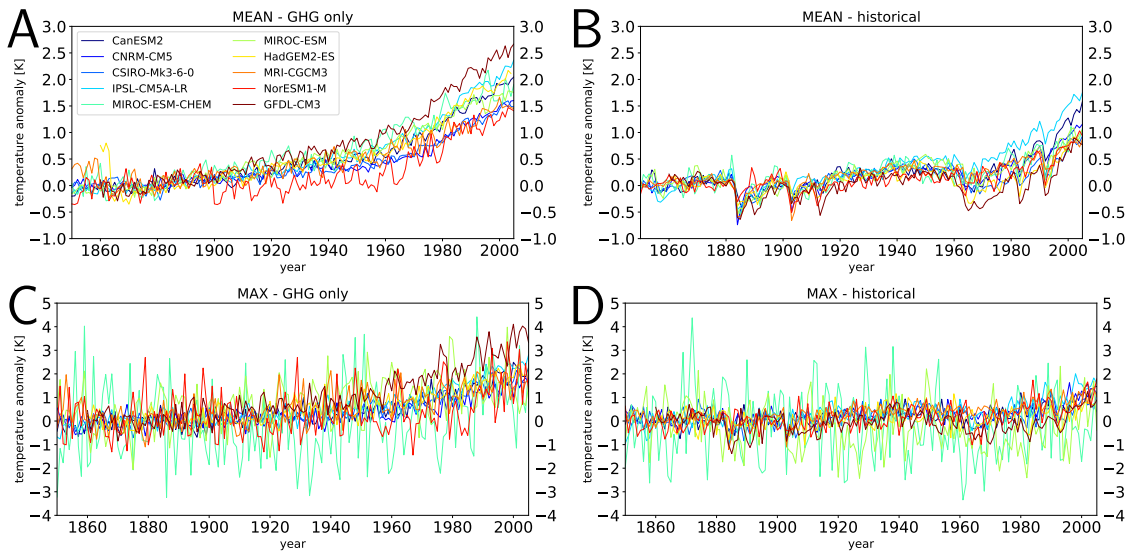


Figure 4: **Time series of global MEAN and MAX temperature comparing GHG (greenhouse gases only) and HIST (historical).** Results are shifted to show the anomaly with the reference period 1860-1890. Those curves are averaged over all available realizations for each model. Some curves are smoother because of a smaller number of realizations.

variability earlier than in a climate without aerosols. NorESM1-M contains only one realization for its GHG experiment, which may leave room for a high coincidental component. CNRM-CM3 on the other hand, contains 6 realizations, so that the number of realizations can not be an explanation for this model's result. The global time series of CNRM-CM3 (see Figure 4) shows similar temperatures for MEAN HIST and GHG in 2005, which points on a small aerosol effect in this model. This could be a reason for the reversed order of global MEAN GHG and HIST TOE. The error bars from this model (see Figure 5A) are huge, so that some realizations might have a different TOE order.

In many cases no MAX HIST TOE is within modelling time span until 2005 (see Figure 5B). Often, there is only a MAX GHG TOE and no MAX HIST TOE (indicated by orange-black ending caps), which leaves open in which year (if any) a MAX HIST TOE would occur and how large the difference between HIST and GHG is. The only models where both HIST and GHG TOE appear are IPSL-CM5A-LR, CSIRO-Mk.3-6-0, CNRM-CM5 and CanESM2. Only CSIRO-Mk.3-6-0 even has a HIST TOE before a GHG TOE, which means, that modelled MAX temperature leaves natural variability earlier in those experiments with aerosols than in the ones with only greenhouse gases. This model includes the carbon-on-snow effect (Boucher et al., 2013), which could be one reason for a higher (less negative) radiative forcing and smaller cooling effect of aerosols, even some warming in in this case.

The model MRI-CGCM3 finds a TOE, already in the first year in 1850 (see Figure 5C). This is, because the time series starts outside of the variability range and stays there for four years. Later, MEAN temperature falls back within variability range and stays low for some decades. Those results show the limits of this TOE definition (see chapter 5, Outlook), because in this case there is a TOE that does not necessarily indicate a climate warming.

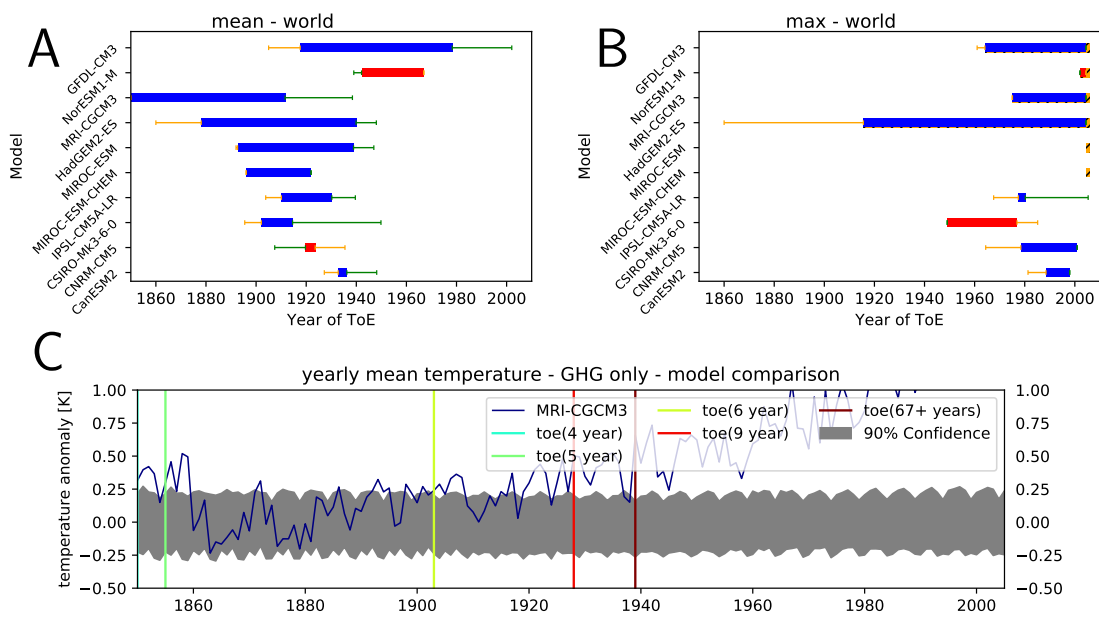


Figure 5: **Global TOE difference of HIST and GHG for each model:** All TOE are averaged over all available realizations. The error bars mark the standard deviation between different realizations. **A and B:** Left end of the blue horizontal bar indicates the year, where a TOE for GHG occurs. The right end of the same bar indicates the corresponding HIST TOE of the same model. For red horizontal bars HIST TOE occurred previous to GHG TOE (left end HIST, right end GHG). If no HIST TOE occurs until the end of 2005, an orange-black ending cap on the right side of the diagram is drawn. Compared to Hawkins and Sutton (2012) here, TOE occur very early, because their reference period is 1986-2005 (here: 1860-1890) **C:** The time series of model MRI-CGCM3 (realization r1i1p1) is shown separately in order to explain the occurrence of GHG TOE already in the first year in 1850.

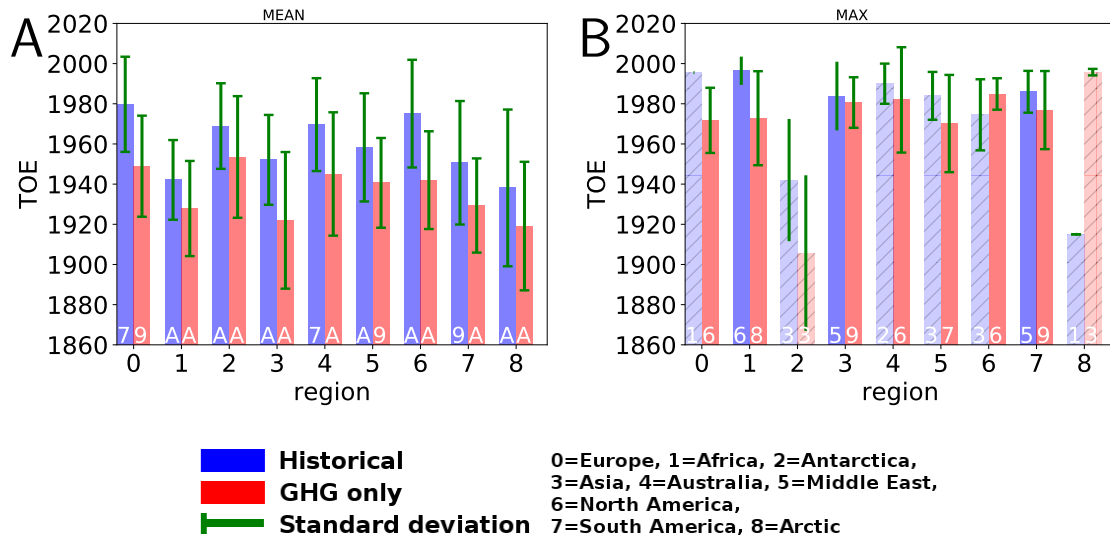


Figure 6: **TOE difference of HIST and GHG for different regions: A: MEAN and B: MAX values.** All TOE years are averages over all models. The number of models, from which a TOE was determined is printed at the bottom of each bar (A = all 10 models). If the number is smaller than 5 (less than 50% of all models), the bar is plotted transparent. The green vertical lines indicate the inter-model standard deviation. Possible discrepancies to Figure 3, regarding the number of models that find a TOE, arise because there the value for  $m$  is fixed during parameter adjustment. Here,  $m$  can be increased according to Chapter 2.4. Late MEAN HIST TOE in Europe confirm the finding of Hawkins and Sutton (2012).

### 3.3 Regional variability

This thesis's TOE findings underlie great differences regarding the region where they occur. Therefore, MEAN and MAX TOE for every continent were investigated separately and the focus is on Europe (region 0 in our label key).

In order to compare models regardless of region it would be pointless to calculate a mean of all regions, since their size and weight in global temperature differs a lot. The only way to reduce values to only model differences is to compare global values, as already done in Figure 5A and B.

As Figure 6A shows, model-averaged MEAN GHG TOE happens earlier than MEAN HIST TOE everywhere. The difference ranges from 14 years (Africa) to 33 years (North America) for MEAN temperature. Hawkins and Sutton (2012) found that in Europe TOE occurs comparatively late, which can be confirmed by the present study, at least in the MEAN HIST experiment.

The MAX temperature (see Figure 6B) shows different behavior. In two regions (North America and Arctic) GHG TOE happens 9 and 81 years later than HIST TOE. North America shows both the highest positive TOE difference in MEAN temperature and a negative TOE difference in MAX temperature. The high MEAN TOE difference could be caused by large aerosol emissions between the 1940s and 1970s (Smith et al., 2011). The negative MAX TOE difference cannot be explained with the available data. The reversed order of MAX TOE years in the Arctic region may be caused by a small warming effect of aerosols due to higher absorption, when falling on white snow ground. Still, the number of models detecting a TOE in the Arctic is too small to confirm this hypothesis. Also, not all models include the carbon-on-snow effect. In general MEAN

temperatures are more reliable than MAX temperature values in this thesis (see Chapter 4). In the other regions the delay of HIST TOE relative to GHG TOE ranges from 3 (Asia) to 36 (Antarctica) years. The inter-model standard deviation (green vertical lines) as a measure of uncertainty overlap in all regions. The results have to be treated carefully for average values calculated from a little number of models. This is the case for most of the HIST experiments. Experiments with less than half of the models detecting a TOE are displayed transparent to indicate less confident values. In those cases more than half of the models do not find any TOE, which means, that their TOE (if any) will happen after 2005. However, the model-averaged value includes only those models with a certain TOE before 2005 and ignores models with later TOE, which potentially diverts averaged TOE to the past.

Albeit Earth is warming globally, there are huge differences in local warming. Especially in high latitudes warming is stronger and variability is higher (Mahlstein et al., 2011) but also the emergence of climate change indicators is delayed. It will be one of the tasks to look whether CMIP5 models reproduce this finding when it comes to TOE investigation. The data on hand is of limited suitability because regional differences are only distinguished by continents and some continents have huge meridional magnitude. Nevertheless, the Arctic (region key 8) and Antarctic (key 2) can be compared to all other regions in order to distinguish high latitudes to the rest of the world. MEAN TOE data is influenced by all temperature zones equally and does not fit the purpose of this comparison. MAX TOE is almost only influenced by the warmest part inside of one region, which is in low latitudes mostly for almost all regions but Arctic and Antarctica. Here, Figure 6B shows for Arctic and Antarctic regions the earliest MAX TOE in HIST experiment, which represents the temperature with greenhouse gases and aerosols, contradicting Mahlstein's results. Although it is important to notice that for the Antarctic region only three and for the Arctic region, only one of all 10 models detect a MAX TOE at all. Variability (shown by green vertical lines, which are inter model standard deviation) of those three models is comparatively high which supports the finding of Mahlstein. The Arctic (key 8) MAX HIST TOE is the earliest of all model-averaged HIST TOE, but it is detected by only one of 10 models. In conclusion the TOE approach rather disagrees with Mahlstein's results, regarding TOE delay in high latitudes. A reason for this diverging result could be, that a signal that is both stronger and delayed can in total be shifted towards the past or the future, depending on whether the strength or the delay dominates the TOE signal. The approach used here can not distinguish between both effects.

The appearance of TOE in small regions is much more stable than for the whole world. Due to high variability on local scales, detection of climate change indication becomes difficult (Stott et al., 2010). Global variability (confidence interval) has a smaller range than regional variability. That is why the global MEAN and MAX temperature tends to leave the 90 % confidence interval several decades earlier, which can be caused by small spikes whereas in regional TOE analysis a strong and long lasting signal is required in order to trigger a new TOE.

In Figure 7 only European time series are shown. Figures 7A and B compare HIST MEAN with GHG MEAN. As expected, MEAN HIST temperature drops in the 1960s whereas MEAN GHG temperature steadily rises for most of the models. The same applies to MAX temperature (see Figure 7C and D), but in a less distinct extent. Compared to the MAX HIST time series for the whole world (see Figure 4D) the 1960 dimming phase is more clear in Europe because the European aerosol emission increase was stronger than in the rest of the world (Smith et al., 2011).

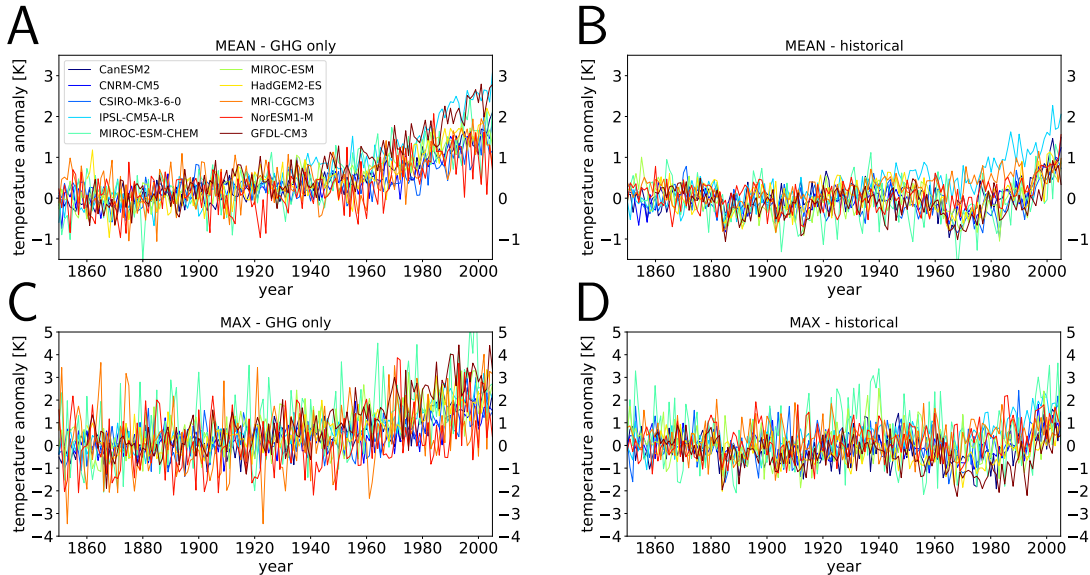


Figure 7: **Time series of European MEAN and MAX temperature for HIST and GHG:** Comparison of all models for Europe only. All available realizations are averaged for each model. **A:** MEAN HIST, **B:** MEAN GHG, **C:** MAX HIST, **D:** MAX GHG. The number of realizations for MEAN and MAX is equal, because they originate from the same experiment run. Both MAX time series show a higher variability than the MEAN time series, because heat waves and extreme temperature events do not occur with a constant frequency.

### 3.4 Differences in models

A deeper look into the influence of aerosols in Europe is provided by Figures 8A-D which compare two models with lowest (MRI-CGCM3) and largest (MIROC-ESM) TOE difference in European MEAN temperature (see Figure 8E). The TOE in Figures A-D may differ slightly from those in Figure E, because for each time series (A-D) only one realization was chosen to be plotted, whereas in E a mean of all realization TOE is displayed, according to Chapter 2.4. For every displayed time series, the one realization was chosen, that shows a TOE as close as possible to the mean of all TOE from all available realizations.

In MRI-CGCM3 (see Figure 8A and B) both HIST and GHG experiments show a distinct temperature rise with GHG developing a TOE (at least 4 consecutive years) 43 years later than HIST. The main reason for leaving variability (grey area) this early is the small range of the variability. The HIST TOE in 1940 may be caused by internal spikes more than a significant out-of-variability temperature rise, because it happens even before the temperature drop in the 1960s and temperature falls back inside the variability range for the following decades. The GHG TOE in 1983 however may indicate a real climate change because the MEAN temperature curve does not fall within variability range again except for one year. This model shows that the chosen TOE approach still is limited and many realizations and models should be compared to get statistical relevant results. Alternatively, the TOE definition could be altered by including the following years in the TOE conditions (see Chapter 5, Outlook).

The MIROC-ESM model shows an expected result, when looking on the realization-averaged TOE difference in Figure 8E. GHG TOE is expected to occur earlier than HIST TOE because of the cooling aerosol effect. Figure 8C shows a warming, most probably caused by greenhouse gases



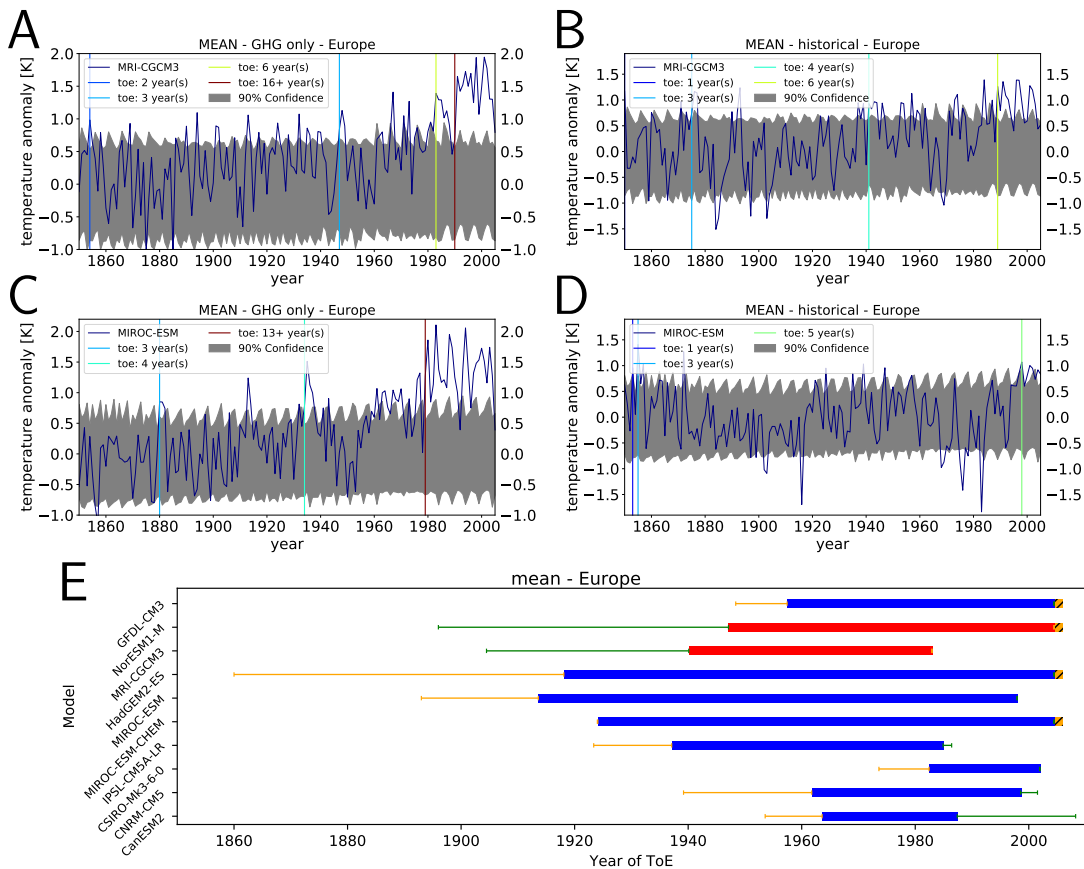


Figure 8: **Comparison of those models with highest and lowest aerosol difference on European MEAN temperature:** Time series with TOE markers for **A:** MRI-CGCM3 (r1i1p1) and GHG, **B:** MRI-CGCM3 (r5i1p2) and HIST, **C:** MIROC-ESM (r3i1p1) and GHG, **D:** MIROC-ESM (r3i1p1) and HIST, **E:** summary of TOE differences in Europe developed by different models. The choice of the realization to plot here was made for reasons of the best demonstration. Right ends of each blue bar indicate HIST TOE, the left ends indicate GHG TOE (vice versa for red bars). The small error bars show the realization standard deviation of GHG TOE (yellow) and HIST TOE (green). 8 of 10 models show a delay (blue bar) of TOE, which is probably caused by increased aerosol emission in the second half of the 20<sup>th</sup> century.

from the year 1950 on, whereas in Figure 8D, temperature stays in a low trend, before it exceeds the upper bound of the variability range in 1998 for 5 years.

A key aspect of this thesis is the investigation of TOE delay, forced by aerosols in the 1950s in Europe. For this purpose, Figure 8E is one of the main achievement results. Eight of ten models find a hypothetical GHG TOE, which happens before a HIST TOE. Those GHG TOE would occur in an ideal model environment without aerosols. Five of these eight models find a delayed HIST TOE between 1985 and 2002. The average TOE delay of all six models, that detect both a HIST and a GHG TOE, with its standard deviation is  $29.5 \pm 41.8$  years. The three remaining of these eight models do not detect any HIST TOE until 2005.

On the other hand, two of 10 models show a HIST TOE that occurs before a GHG TOE can happen, which contradicts the expectation resulting from the cooling aerosol effect. In one of those two (NorESM1-M) no GHG at all happens until 2005 and the other one (MRI-CGCM3) was already discussed in this chapter.

A full summary and comparison of all models and all regions is shown in Figure 9. For MEAN temperature (9A) most models show a delayed HIST TOE, compared to GHG TOE in the majority of regions. Sometimes no HIST TOE but only GHG TOE are found. Noticeably, an exception make MRI-CGCM3 and NorESM1-M, where in seven of nine regions GHG TOE (if any) happens past HIST TOE and only in two, respectively one region(s) the reversed order is found. Both models appear to simulate a rather weak temperature increase in total (see Figure 4A and B on page 12). Especially for NorESM1-M the increasing phase in the GHG experiment starts late in the 1960s (compare Figure 4A), whereas other models show a continuously rising temperature from the beginning of the 20<sup>th</sup> century on. So, the climate warming signal in GHG experiment is delayed, resulting in reversed orders in MEAN GHG and HIST TOE (see Figure 9A).

It is clearly visible that MAX temperature TOE often is reached within modelling time span only for GHG experiments, especially in the following models: MIROC-ESM, HadGEM2-ES, NorESM1-M and GFDL-CM3. In case of GFDL-CM3 it is notable, that Allen et al. (2013) already detected a very large dimming trend in this model, which prevents TOE to be called. However, as Golaz et al. (2013) found out, in this model the aerosol effect is overestimated. Because of this overestimation, a strong ocean warming effect is caused, which is a highly debatable statement and the TOE results of this model's historical experiment should be treated with caution. Another exception is made by IPSL-CM5A-LR, which generates 17 out of a possible maximum of 18 TOE. This model in both GHG (see Figure 9A) and HIST (9B) concludes with one of the two highest temperatures in the last modelled year 2005 (compare Figure 4 on page 12). Higher modelled temperatures increase the probability of a TOE occurrence, because TOE rely on temperatures exceeding background noise and this noise is generated from a fixed forcing in the year 1850.

An unexpected result is achieved by NorESM1-M, where a global HIST TOE occurs in 1942 and a GHG TOE follows 25 years later (remember Figure 5 on page 13). Figure 10 shows the time series of this model. For each time series a realization was chosen, that calls its TOE similar to the realization-averaged TOE in Figure 5A. The overall warming is weakened in the HIST experiment, but still the TOE (at least 4 consecutive years) is shifted towards the past. One reason is the different smoothness of both curves. HIST TOE is triggered by a small peak whereas GHG TOE occurs directly before a distinct warming trend. In general, this model does not show any obvious temperature drop in the 1950s, but only a distinct temperature rise from the 1960s on.

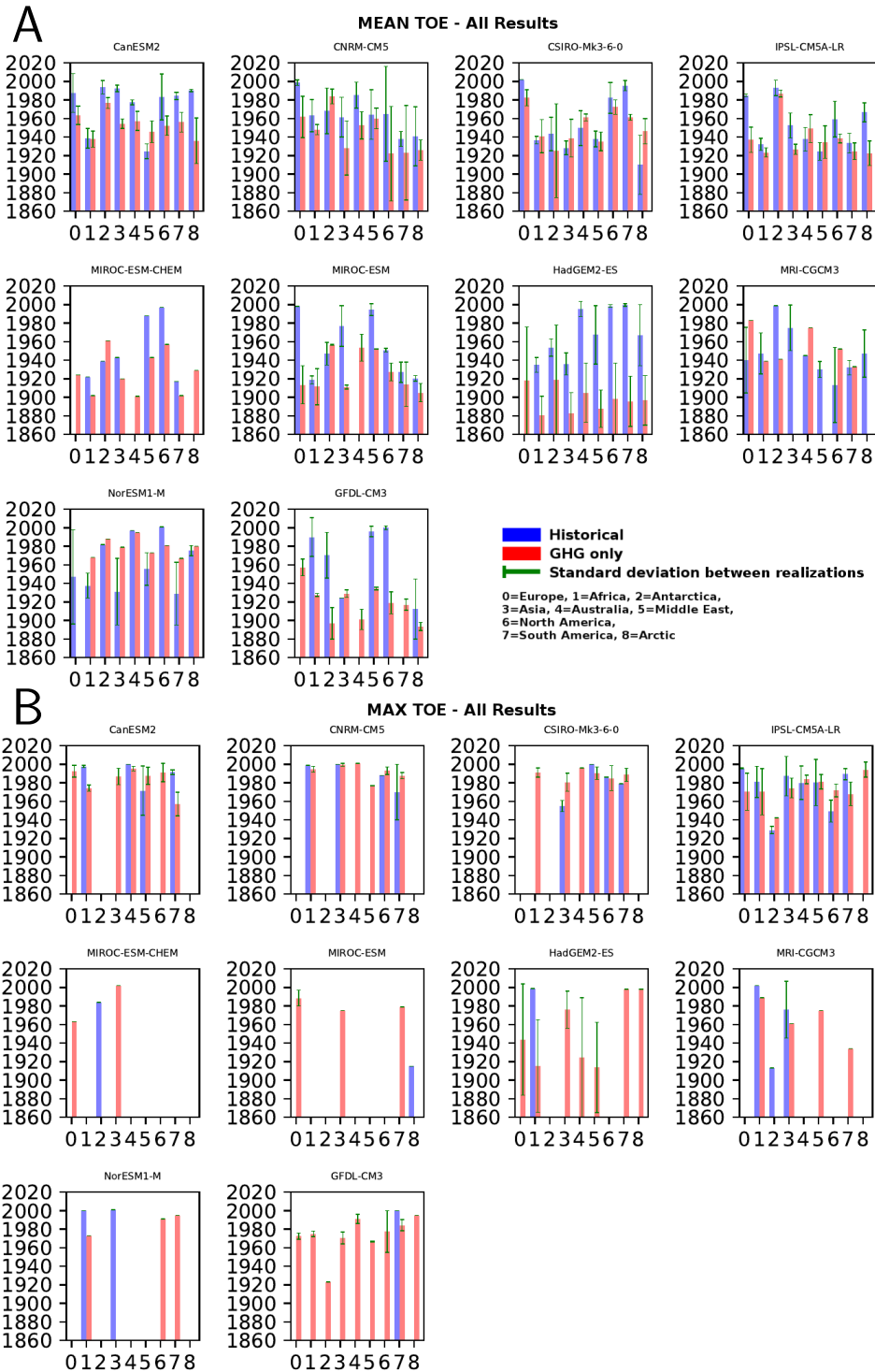


Figure 9: **TOE summary for all regions and all models: A: TOE for MEAN temperature, B: TOE for MAX temperature.** In almost all experiments GHG TOE is called previous to HIST TOE. Only MEAN HadGEM2-ES shows predominantly earlier HIST TOE than GHG TOE.

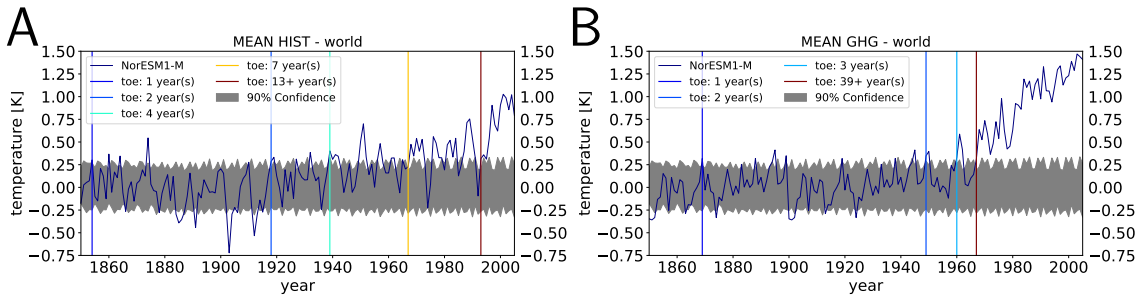


Figure 10: **Time series of NorESM1-M Global HIST (r3i1p1) and GHG (r1i1p1): A: HIST and B: GHG values.** In this model HIST TOE (at least 4 consecutive years) occurs previous to GHG TOE. Also the GHG curve appears smoother than the HIST curve.

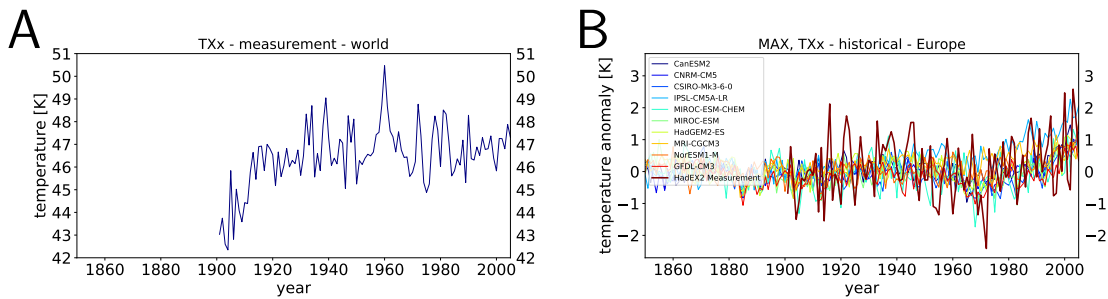


Figure 11: **Time series of HadEX2 observation with model comparison: A: global TXx (hottest daily maximum) temperature observation.** Please remember the different regional availability of global observation data. **B: comparison of Europe modelled MAX and measured TXx.** The model curves are averaged over all realizations. The observation curve here is shifted arbitrarily in order to fit it to the model curves.

### 3.5 Reliability of CMIP5 models

Figure 11 shows the HadEX2 measurement (Donat et al., 2013) for the whole globe (A) and Europe only (B). European measurement is compared to the European part of the CMIP5 models (see Table 2).

Measurement time series can be created for certain regions, but confidence in those results is limited. This is because of different availability for different regions during measurement time (Donat et al., 2013). On the other hand, time series that include all grid points around the globe have to be treated carefully because in the first decades regions with huge impact on global maximum temperature are missing. The longest time span in HadEx2 is available for Europe and North America, beginning in year 1901. Large parts of Asia join in 1936 (India 1957). Please note, that model and measurement show different parameters. The modelled max value is the highest mean temperature of all daily mean temperatures in each year, whereas the measured TXx value is the maximum temperature of the hottest day in each year. Still, the comparison holds for a first guess and validates the warming trend during the last decades as well as a local minimum in temperature extremes in the second half of the last century, which is probably caused by the increased aerosol emissions at that time. Furthermore, the local minimum is more distinctly visible in European measurement curve (B) than in the world (A), which confirms the cooling effect of aerosols predominantly in Europe (Smith et al., 2011).

The comparison between aerosol forcing, stated in the IPCC-AR5 and this thesis's results is an

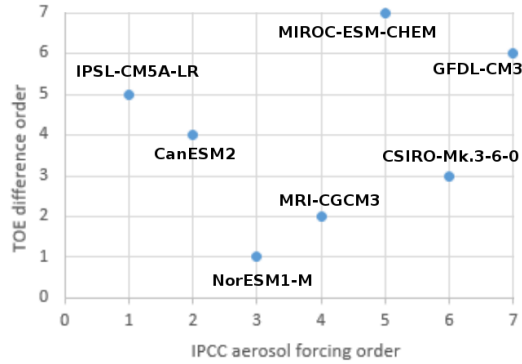


Figure 12: **Scatter plot IPCC aerosol forcing vs. TOE difference:** Models were sorted by ERFari+aci (IPCC) and TOE respectively and their order was compared in a scatter plot.

approach in evaluating TOE difference as a measure of aerosol influence. Therefore, in Figure 12 models were sorted by TOE difference and plotted in a scatter plot versus the order of ERFari+aci from the IPCC-AR5. The numbers on x and y axis represent the order of TOE difference (x) and ERFari+aci (y) of those 6 models which can be found both in the used CMIP5 ensemble and the IPCC-AR5 report. There is no significant correlation in Figure 12. So probably the TOE difference can not be used as a quantitative measure of aerosol effect in a model, at least not in the way it is done here. Still, the TOE delay can be used qualitatively, to determine how aerosols influence the occurrence of modelled climate warming signals.

## 4 Discussion

### 4.1 Possible causes of disagreement

Differences in models are one of the main aspects that need to be held responsible for ambiguous results. HadGEM2-ES starts in 1859, all other models in 1850. Furthermore, grid size varies from 64x128 to 160x320 (see Table 1) which leads to uncertainties, especially for warm regions, that could influence the MAX value.

One CMIP5 model (NCAR/CCSM4) had to be excluded from TOE analysis because the control run's length (156 years) does not allow calculating a proper percentile. An additional length of at least 100 years more is necessary. This number results from the 5-year shift and the 95 %-percentile approach which needs at least 20 aligned control run slices to compare (see Chapter 2.3 for details on the calculation of confidence intervals.).

As explained in Chapter 2.4, TOE is defined as a signal, which is outside of the 90 % confidence interval for at least 4 consecutive years. Other groups chose different definitions. Some of those definitions were tested in the process of this thesis. A TOE which was called by a single signal-to-noise ratio of 2.0, would occur mostly very late and would leave us with many runs, which do not raise any TOE at all. A second approach was to satisfy a TOE by having only  $m$  out of 10 consecutive years outside of the confidence interval. Doing so, many TOE in very early years were encountered but not any regularity regarding the aerosol effect were detected due to a large coincidental impact on the results. The agreement with four consecutive years is a conservative choice, but still leaves room for disproof of the main thesis.

In order to compare different models and regions, the temperature anomaly rather than absolute temperature was object of investigation. The reference time period plays a crucial role in TOE analysis. The first idea of taking the mean from 1880 to 1980 as reference period led to the problem of getting very early TOE. Especially HIST experiments started with high anomalies, because the 1950 local temperature minimum lowers the mean temperature which leads to higher anomalies for the whole time span. So it happened, that many TOE were called in the end of the 19<sup>th</sup> century because of higher temperature anomalies relative to the comparatively low temperatures later in the 20<sup>th</sup> century.

### 4.2 Conclusion

In general MEAN values qualify for more distinct results than MAX values. Temperature extreme events like heatwaves have more coincidental aspects than mean values and so, TOE analysis which relies on reproducibility sometimes becomes unstable and inconsistent. Nevertheless, extreme events play a crucial role in indicating climate change processes which is why were included in this thesis with particular attention.

In global analysis, the majority of models find TOE very early, which is due to the smaller variability range on global scales, compared to local scales. The small variability range causes a small confidence interval and so, small peaks can already lead to the occurrence of a TOE.

All in all, the results measure up to the expectation. Aerosols cause a delay of TOE in most models and most regions, due to their cooling effect. This can be interpreted as follows: Because of increasing aerosol emission in the course of the industrial growth in the second half of the last

century, global warming has been slowed down. Still, the aerosol effect is not known as good as the greenhouse effect. An aerosol effect that is higher than assumed until now would mean, that the greenhouse effect on the other hand must be higher than assumed until now as well. The delaying effect of aerosols can be seen within the CMIP5 models as shown in the present thesis.

## 5 Outlook

The achievements of this study can be improved by changes in definitions and additional analysis. In further investigation the TOE definition should be extended to exclude more systematic biases. One idea is to allow only those TOE where at least 50 % of all following years are outside of the confidence interval. So, TOE are detained to be called by multi-year peaks.

The background variability could be designed smoother, by calculating the 5<sup>th</sup> and 95<sup>th</sup> percentile not from aligned slices as explained in Chapter 2.3 but from one whole range of the control experiment. The approach with different slices is also possible, because the number of years included in all models is sufficiently high, but a certain dependence of the confidence interval on the number of control years can not be ruled out.

In order to investigate TOE difference depending on latitude, future studies should implement a function able to distinguish between coordinate ranges instead of only continents.

## List of Figures

1	Visualization of region boundaries . . . . .	6
2	Visualization of variability range . . . . .	7
3	Parameter adjustment for $m$ in Europe . . . . .	8
4	Global MEAN, MAX, HIST, GHG temp time series comparison . . . . .	12
5	Global TOE difference of HIST and GHG . . . . .	13
6	Regional variability in HIST and GHG TOE . . . . .	14
7	Europe HIST and GHG temp time series from all models . . . . .	16
8	Europe HIST and GHG temp time series from MRI-CGCM3 and MIROC-ESM . . . . .	17
9	TOE summary for all regions and all models . . . . .	19
10	Global HIST and GHG temp time series from NorESM1-M . . . . .	20
11	Global observation temp time series of HadEX2 . . . . .	20
12	Scatter plot IPCC aerosol forecing vs. TOE difference . . . . .	21

## List of Tables

1	List of CMIP5 models . . . . .	5
2	List of regions, their extent and boundaries . . . . .	6
3	Parameter adjustment: Number of encountered TOE . . . . .	10
4	Parameter adjustment: Average TOE depending on $m$ . . . . .	11



## References

- Allen, R., Norris, J., and Wild, M. (2013). Evaluation of multidecadal variability in cmip5 surface solar radiation and inferred underestimation of aerosol direct effects over europe, china, japan, and india. *Journal of Geophysical Research: Atmospheres*, 118(12):6311–6336. doi:10.1002/jgrd.50426.
- Arora, V., Scinocca, J., Boer, G., Christian, J., Denman, K., Flato, G., Kharin, V., Lee, W., and Merryfield, W. (2011). Carbon emission limits required to satisfy future representative concentration pathways of greenhouse gases. *Geophysical Research Letters*, 38(5). doi:10.1029/2010GL046270.
- Bador, M., Terray, L., and Boé, J. (2016). Emergence of human influence on summer record-breaking temperatures over europe. *Geophysical Research Letters*, 43(1):404–412. doi:10.1002/2015GL066560.
- Bellouin, N., Collins, W., Culverwell, I., Halloran, P., Hardiman, S., Hinton, T., Jones, C., McDonald, R., McLaren, A., O’Connor, F., et al. (2011). The hadgem2 family of met office unified model climate configurations. *Geoscientific Model Development*, 4(3):723–757. doi:10.5194/gmd-4-723-2011.
- Bentsen, M., Bethke, I., Debernard, J., Iversen, T., Kirkevåg, A., Seland, Ø., Drange, H., Roe-landt, C., Seierstad, I., Hoose, C., et al. (2012). The norwegian earth system model, noresm1-m-part 1: Description and basic evaluation. *Geoscientific Model Development Discussions*, 5:2843–2931. doi:10.5194/gmdd-5-2843-2012.
- Boer, G., Flato, G., and Ramsden, D. (2000). A transient climate change simulation with greenhouse gas and aerosol forcing: projected climate to the twenty-first century. *Climate Dynamics*, 16(6):427–450. doi:10.1007/s003820050338.
- Boucher, O., Randall, P., Artaxo, D., Bretherton, C., Feingold, G., Forster, P., Kerminen, V., Kondo, Y., Liao, H., Lohmann, U., Rasch, P., Satheesh, S., Sherwood, S., Stevens, B., and Zhang, X. (2013). Clouds and aerosols. in: *Climate change 2013: The physical science basis. contribution of working group i to the fifth assessment report of the intergovernmental panel on climate change*. doi:10.1017/CBO9781107415324.016.
- Collier, M., Jeffrey, S. J., Rotstayn, L. D., Wong, K., Dravitzki, S., Moseneder, C., Hamalainen, C., Syktus, J., Suppiah, R., Antony, J., et al. (2011). The csiro-mk3. 6.0 atmosphere-ocean gcm: participation in cmip5 and data publication. In *International Congress on Modelling and Simulation—MODSIM*.
- Donat, M., Alexander, L., Yang, H., Durre, I., Vose, R., Dunn, R., Willett, K., Aguilar, E., Brunet, M., Caesar, J., et al. (2013). Updated analyses of temperature and precipitation extreme indices since the beginning of the twentieth century: the hadex2 dataset. *Journal of Geophysical Research: Atmospheres*, 118(5):2098–2118. doi:10.1002/jgrd.50150.

- Donner, L. J., Wyman, B. L., Hemler, R. S., Horowitz, L. W., Ming, Y., Zhao, M., Golaz, J.-C., Ginoux, P., Lin, S.-J., Schwarzkopf, M. D., et al. (2011). The dynamical core, physical parameterizations, and basic simulation characteristics of the atmospheric component am3 of the gfdl global coupled model cm3. *Journal of Climate*, 24(13):3484–3519. doi: 10.1175/2011JCLI3955.1.
- Dufresne, J.-L., Foujols, M.-A., Denvil, S., Caubel, A., Marti, O., Aumont, O., Balkanski, Y., Bekki, S., Bellenger, H., Benshila, R., et al. (2013). Climate change projections using the ipsl-cm5 earth system model: from cmip3 to cmip5. *Climate Dynamics*, 40(9-10):2123–2165. doi:10.1007/s00382-012-1636-1.
- Giorgi, F. and Bi, X. (2009). Time of emergence (toe) of ghg-forced precipitation change hot-spots. *Geophysical Research Letters*, 36(6). doi: 10.1029/2009GL037593.
- Golaz, J.-C., Horowitz, L. W., and Levy, H. (2013). Cloud tuning in a coupled climate model: Impact on 20th century warming. *Geophysical Research Letters*, 40(10):2246–2251. doi:10.1002/grl.50232.
- Hawkins, E. and Sutton, R. (2012). Time of emergence of climate signals. *Geophysical Research Letters*, 39(1). doi:10.1029/2011GL050087.
- Hourdin, F., Foujols, M.-A., Codron, F., Guemas, V., Dufresne, J.-L., Bony, S., Denvil, S., Guez, L., Lott, F., Ghattas, J., et al. (2013). Impact of the lmdz atmospheric grid configuration on the climate and sensitivity of the ipsl-cm5a coupled model. *Climate Dynamics*, 40(9-10):2167–2192. doi:0.1007/s00382-012-1411-3.
- Lobell, D. B. and Burke, M. B. (2008). Why are agricultural impacts of climate change so uncertain? the importance of temperature relative to precipitation. *Environmental Research Letters*, 3(3):034007. doi:10.1088/1748-9326/3/3/034007.
- Mahlstein, I., Knutti, R., Solomon, S., and Portmann, R. (2011). Early onset of significant local warming in low latitude countries. *Environmental Research Letters*, 6(3):034009. doi:10.1088/1748-9326/6/3/034009.
- Mitchell, J. F., Johns, T., Gregory, J. M., and Tett, S. (1995). Climate response to increasing levels of greenhouse gases and sulphate aerosols. *Nature*, 376(6540):501–504. doi:10.1038/376501a0.
- Sillmann, J., Pozzoli, L., Vignati, E., Kloster, S., and Feichter, J. (2013). Aerosol effect on climate extremes in europe under different future scenarios. *Geophysical Research Letters*, 40(10):2290–2295. doi:10.1002/grl.50459.
- Smith, S. J., Aardenne, J. v., Klimont, Z., Andres, R. J., Volke, A., and Delgado Arias, S. (2011). Anthropogenic sulfur dioxide emissions: 1850–2005. *Atmospheric Chemistry and Physics*, 11(3):1101–1116. doi:10.5194/acp-11-1101-2011.
- Stanhill, G. and Cohen, S. (2001). Global dimming: a review of the evidence for a widespread and significant reduction in global radiation with discussion of its probable causes and possible agricultural consequences. *Agricultural and forest meteorology*, 107(4):255–278. doi:10.1016/S0168-1923(00)00241-0.

- Stott, P. A., Gillett, N. P., Hegerl, G. C., Karoly, D. J., Stone, D. A., Zhang, X., and Zwiers, F. (2010). Detection and attribution of climate change: a regional perspective. *Wiley Interdisciplinary Reviews: Climate Change*, 1(2):192–211. doi:10.1002/wcc.34.
- Voldoire, A., Sanchez-Gomez, E., y Méliá, D. S., Decharme, B., Cassou, C., Sénési, S., Valcke, S., Beau, I., Alias, A., Chevallier, M., et al. (2013). The cnrm-cm5. 1 global climate model: description and basic evaluation. *Climate Dynamics*, 40(9-10):2091–2121. doi:0.1007/s00382-011-1259-y.
- Watanabe, S., Hajima, T., Sudo, K., Nagashima, T., Takemura, T., Okajima, H., Nozawa, T., Kawase, H., Abe, M., Yokohata, T., et al. (2011). Miroc-esm 2010: model description and basic results of cmip5-20c3m experiments, *geosci. model dev.*, 4, 845–872. doi: 10.5194/gmd-4-845-2011.
- Yukimoto, S., Adachi, Y., Hosaka, M., Sakami, T., Yoshimura, H., Hirabara, M., Tanaka, T. Y., Shindo, E., Tsujino, H., Deushi, M., et al. (2012). A new global climate model of the meteorological research institute: Mri-cgcm3—model description and basic performance—. *Journal of the Meteorological Society of Japan. Ser. II*, 90:23–64. doi:10.2151/jmsj.2012-A02.

# Acknowledgement

I would like to say thank you to all the people who supported me during the creation of this Bachelor thesis. First I want to express my gratefulness to my supervisor Marc Salzmann. Thank you for your patience, the contribution of your knowledge and your kind advice in all forms. Thank you to Johannes Quaas for letting me write my thesis in his group and for the offered help. Last but not the least, I would like to thank my family and friends for their mental assistance.

# Declaration of authorship

Ich versichere, dass ich die vorliegende Arbeit selbständig verfasst und keine anderen als die angegebenen Quellen und Hilfsmittel benutzt habe. Alle Stellen, die wörtlich oder sinngemäß aus veröffentlichten oder noch nicht veröffentlichten Quellen entnommen sind, sind als solche kenntlich gemacht. Diese Arbeit ist in gleicher oder ähnlicher Form noch bei keiner anderen Prüfungsbehörde eingereicht worden.

Leipzig, 30. Oktober 2017

Unterschrift:

---